Concentration dependence of critical scattering from Cr(V) alloys above the Néel temperature

D. R. Noakes
Physics Department, Virginia State University, Petersburg, Virginia 23806

Eric Fawcett
Physics Department, University of Toronto, Toronto, Ontario, Canada M5S 1A7

T. M. Holden
AECL Research, Chalk River, Ontario, Canada K0J 1J0

(Received 4 November 1996)

We have measured triple-axis neutron scattering data for a single crystal of Cr+0.5 at. % V, in the paramagnetic state above the Néel transition. The data are well fit by a critical magnetic scattering model involving a form of critical susceptibility proposed by Sato and Maki, and the results compared to those for single crystals of chromium and Cr+0.2 at. % V. All of the results are generally consistent with a critical exponent $\nu \approx 0.7$. Magnetic stiffness evolves smoothly over the range of alloy concentration studied, but the amplitude scale of the critical fluctuations is more complicated, dropping by more than a factor of 2 between pure chromium and 0.2 at. % V, the region of the magnetic tricritical point and onset of local moments, but then changing little between 0.2 and 0.5 at. % V. [S0163-1829(97)02618-0]

I. INTRODUCTION

Chromium has a simple bcc crystal structure, yet displays complicated magnetic behavior.[1] When cooled through the Néel temperature (T_N) of $\simeq 311$ K it enters an incommensurate spin-density-wave (SDW) state in which the polarization is transverse to the incommensurate-ordering wave vector, $\mathbf{Q}_o$, down to a spin-flip temperature of $\simeq 123$ K, below which the polarization is longitudinal. $\mathbf{Q}_o$ is directed along a cube axis, and the incommensurability is attributed to the magnetic interaction between conduction electrons on nearly parallel pieces of the Fermi surface, which nest when translated through $\mathbf{Q}_o$.[2] This makes chromium an ''itinerant'' antiferromagnet. The characteristics of the magnetic ordering change rapidly when alloyed with other elements, providing a rich array of magnetic properties to study.[3] Attention has naturally focused on the alloys of chromium with vanadium and manganese, adjacent elements in the periodic table.[4] These cause the gentlest disturbance to the band structure, and in a first approximation, simply move the Fermi level down or up.[5,6]

The weak first-order (jump) transition at the Néel temperature of chromium[7] has made it difficult to interpret what appear to be critical phenomena that normally would only be associated with a continuous transition.[1] Among other things, magnetic excitations have been observed near and above T_N by neutron scattering: well defined but not well understood ''Fincher-Burke'' excitations[8] persist up to T_N with, if anything, increasing intensity with temperature, but are not seen in the paramagnetic phase, and a broad spectrum of scattering appears as T_N is approached from below, which persists to temperatures far above the transition.[9] This latter was shown recently[10] to originate at all six satellite positions (including ''silent'' satellites) even in a sample having a single-SDW wave vector.

It has been known for some time that the addition of only a small amount of manganese sends the wavelength of the incommensurability to infinity, creating (simple antiferromagnetic) ''commensurate SDW'' ordering with a continuous transition at considerably higher T_N. The critical behavior of the magnetic excitations observed by neutron scattering near that transition was clearly established.[11] Later it was found that the addition of small amounts (less than 0.2 at. %) of vanadium to chromium, slightly decreasing the wavelength of the incommensurability, reduces the first-order jump to zero, leaving a true continuous transition (not just a disorder-broadened first-order one) to the incommensurate SDW.[12] This indicates that there is a tricritical point on the Néel transition line of the alloy magnetic phase diagram between zero and 0.2 at. % V.

We began to study triple-axis neutron scattering near the continuous Néel transitions in dilute Cr(V) alloys, because these continuous transitions should have truly critical fluctuations and correlations associated with them. We have previously published briefly on a comparison of single crystals of Cr+0.2 at. % V and pure chromium.[13] In those publications, we argued that all the elastic and inelastic scattering observed immediately above T_N *in both samples* is consistent with critical scattering associated with a second-order transition of an itinerant magnet. The only modification of the standard form of critical generalized magnetic susceptibility normally used for commensurate ordering is the replacement of the standard second-order (leading term) polynomial for the ''self-energy'' of a fluctuation as a function of wave vector with a fourth-order polynomial suggested by Sato and Maki[5] that more correctly represents the symmetry around the nearby commensurate (100) position. This is necessary when the ordering wave vector is so close to commensurate that fluctuations associated with distinct (but symmetry-related) ordering wave vectors overlap with significant intensity at (100). This report extends this analysis to measurements on a single crystal of Cr+0.5 at. % V.

To be able to compare the intensity of observed scattering between samples, and thus to determine changes in intensity of the critical scattering with changes in vanadium content, absolute intensities of scattering from these samples in the apparatus were determined by measuring the known cross sections per atom for phonon scattering (near nuclear Bragg peaks) and incoherent elastic scattering (at positions remote from both nuclear structure and magnetic ordering peaks). For each sample, the two cross-section measurements gave essentially the same normalization factor for converting counts per neutron exposure to cross section per atom. We do not see any practical way of defining a physically significant yet model-independent ''intensity of critical scattering'' that can be compared between samples of different compositions. The Sato-Maki model (described below) temperature-independent intensity scale χ^0/r^2, however, drops by more than a factor of 2 between pure chromium and Cr+0.2 at. % V,[13] yet then, as reported below, changes hardly at all between the latter and Cr+0.5 at. % V. This behavior is not yet understood.

II. THEORY

In the triple-axis (energy-resolved) cross section for magnetic scattering of thermal neutrons from the electrons in a sample,[14] using the critical generalized susceptibility of an itinerant-electron system at temperature T approaching a second-order magnetic ordering transition from above, as derived by Izuyama *et al.*,[15] the scattering function for momentum transfer $\mathbf{Q}$ and energy transfer $\hbar\omega$ becomes

$$S(\mathbf{Q},\omega,T)=\frac{N}{(g_J\mu_B)^2}\left(\frac{\omega}{1-\exp(-\hbar\omega/kT)}\right)\times\frac{(\chi^0/r^2)A^2}{A^4[\kappa^2(T)+R(\mathbf{Q})]^2+\omega^2} \quad (1)$$

(see Sato and Maki[5]), where N is the number of scatterers, χ^0 is the strength of the susceptibility of the electron gas without the interaction that causes the ordering, r is the range of the interaction, A^2 is the magnetic stiffness,[14] $\kappa(T)$ is the inverse critical correlation length (which should go to zero at T_N as a power law with critical exponent ν), and $R(\mathbf{Q})$ is the real part of the self-energy of a fluctuation having wave vector $\mathbf{Q}$ (Ref. 13) and is a non-negative function that is zero at the ordering wave vector $\mathbf{Q}_o$. Note that in this formulation, χ^0 cannot be separated from r; together they form a temperature-independent amplitude scale for the critical scattering.

For a divergence point $\mathbf{Q}_o$, isolated in reciprocal space, it is appropriate to take $R(\mathbf{Q})$ to be the simplest possible polynomial, $R(\mathbf{Q})=(\mathbf{Q}-\mathbf{Q}_o)^2$. We attempted to fit this isolated-singularity model to our original triple-axis neutron scattering data from the paramagnetic state of Cr+0.2 at. % V, as a sum of six functions like Eq. (1) centered at the symmetry-related ordering wave vectors, with unacceptably poor results, because the singularities are in fact not isolated. Chromium and its dilute alloys are long-wavelength incommensurate antiferromagnets. In reciprocal space, the ordering wave vector $(Q_o,0,0)=(1-\delta,0,0)$ is separated from the commensurate (100) position by only a small ''incommensurability'' $\delta\ll 1$ rlu (reciprocal lattice unit), as are five other symmetry-related ordering wave vectors: $(1+\delta,0,0)$, $(1,\pm\delta,0)$, and $(1,0,\pm\delta)$, in other Brillouin zones. Symmetry constraints apply to fluctuations on and near the zone boundaries which are ignored by the isolated model. Sato and Maki[5] noted that the sixfold symmetry around the (100) position can be properly represented by a fourth-order polynomial for $R(\mathbf{Q})$ that can only be expressed simply in terms of $\mathbf{q}'=\mathbf{Q}-(100)$, whence

$$R(\mathbf{q}')=\lambda_1[(|\mathbf{q}'|^2-\delta^2)^2+\lambda_2(\{q_x'q_y'\}^2+\{q_y'q_z'\}^2+\{q_z'q_x'\}^2)], \quad (2)$$

where λ_1 is a scale factor (which can be absorbed into other scale parameters) and λ_2 provides the cubic anisotropy around (100). This is the simplest such polynomial possessing such desirable features as only squares of components of $\mathbf{q}'$ with respect to the cubic axes, continuous derivatives across (100), and zeros at the six satellite positions. Assuming $R(\mathbf{q}')$ isotropic for small deviations from any one of the six minima requires $\lambda_2=4$. Then λ_1 can be chosen to be $1/(4\delta^2)$ to make $R(\Delta\mathbf{q}')=|\Delta\mathbf{q}'|^2$ for small deviations $\Delta\mathbf{q}'$ from any minimum. This Sato-Maki model did fit our Cr +0.2 at. % V and pure chromium data well,[13] in spite of the latter's weak first-order transition. To our knowledge, our application of this model to chromium and Cr(V) alloys is the only unified and simultaneous analysis of both the static and dynamic critical magnetic correlations accessible in neutron scattering near a magnetic ordering transition.

There have been some reports that the magnetic scattering in the paramagnetic state of chromium is commensurate diffuse, or has a commensurate diffuse contribution.[9] The Sato-Maki model described here has no independent commensurate part, but the strength of the scattering at the commensurate position relative to the incommensurate peak is energy dependent. $A^2R(\mathbf{q}')$ has units of energy, and can be considered to be the energy cost of creating a mode of wave vector $\mathbf{q}'$, relative to a mode at the (incipient) ordering wave vector. The relative energy of a commensurate mode is $A^2\delta^2/4$ (for pure chromium, about 1.3 THz). For energy less than this, the response at the incommensurate ordering points is much stronger than at the commensurate position, but if probed at $\omega\gg(A^2\delta^2/4)$, little difference can be seen between commensurate and ordering wave vectors, and the scattering will be broadly commensurate. Also, the spectrometer resolution function must be folded with the cross section to produce the observed scattering intensity, as described below.

III. EXPERIMENT AND DATA

The lozenge-shaped Cr+0.5 at. % V single crystal (approximately 3 cm×1 cm×0.7 cm) was mounted in a cryostat on the N5 triple-axis crystal spectrometer of the NRU reactor at AECL Chalk River. Si(111) planes were used as both monochromator and analyzer, and a pyrolytic graphite filter was mounted in the scattered beam, which had a fixed wavelength of 2.37 Å. Data were collected near the (010) reciprocal lattice position in the (001) plane. Vertical slits of height 2.5 cm were mounted before the sample and detector to limit vertical divergence to 1.0° and exclude direct scattering from the $(0,1,\pm\delta)$ incommensurate SDW ordering

positions above and below the spectrometer plane. In the paramagnetic state, however, scattering intensity centered on those positions is diffuse, extending into the plane of the spectrometer, and must be included in the resolution-folding analysis described below.

To characterize the spectrometer resolution, and allow absolute intensity calibration, a number of control scans were taken: constant-**Q** scans of incoherent-elastic scattering from the sample and from pure vanadium mounted in place of the sample, constant-**Q** scans of several low-energy phonons in the sample, and elastic scans to determine the elastic half-maximum ellipse (in the spectrometer plane) of the $(0,1-\delta,0)$ magnetic Bragg peak about 7 K below T_N. This latter is crucial in determining the in-plane ''mosaic spread'' of the sample, without being misled by extinction in much stronger nuclear Bragg peaks.

It is not possible to determine the transition temperature by sitting at a single reciprocal space position and monitoring intensity as a function of temperature, because the position of most intense scattering is itself a function of temperature. To determine T_N, short elastic scans through ordering wave vector positions were executed while warming and cooling through the transition. During these studies, weak additional Bragg peaks due to a small amount of an impurity phase were discovered at slightly smaller incommensurability than the main magnetic Bragg peaks. While the main incommensurate Bragg peaks disappear at $T_N=261$ K (leaving diffuse paramagnetic critical scattering), the impurity-phase Bragg peaks persist to at least 290 K, but are significantly weaker there. The impurity-phase Bragg peak intensity variation with temperature ($T_{N,i}\approx 293$ K) and δ_i are consistent with less than 10% of the sample volume being chromium with much less than 0.2 at. % vanadium in it.

While the impurity-phase $(100)_i$ axes were well aligned with the main-phase (100) axes, the impurity-phase $(010)_i$ axes were tipped somewhat out of the spectrometer plane, so that near $(0,1\pm\delta_i,0)$, the impurity-phase Bragg intensity was approximately a factor of 10 weaker, and did not begin to compete with even elastic critical scattering from the main phase until more than 5 K above T_N (as discussed below). All elastic scattering data for the critical scattering analysis below were therefore taken near $(0,1\pm\delta,0)$. Then the existence of the weak impurity-phase Bragg peaks complicates the analysis, but it is still tractable when the temperature is far enough below $T_{N,i}$ that there is no significant impurity-phase critical (diffuse) scattering intensity. Sequences of short elastic scans across $(0,1-\delta,0)$ with small temperature increments (warming and cooling) indicated that the full width at half maximum (FWHM) increased suddenly at $T_N=261.1\pm0.1$ K, while the intensity evolves smoothly (the transition is continuous).

To investigate the complete energy-dependent critical scattering a number of scans were taken at each of several selected temperatures above T_N. At each selected temperature, after a temperature equilibration time of order 1 h, radial elastic and constant energy transfer scans were taken through $(0,1\pm\delta,0)$ and the commensurate position. Some constant-E transverse scans were also taken to control transverse resolution effects in fitting (below). Additionally, constant-**Q** scans were taken at (010) and near the $(0,1-\delta,0)$ elastic intensity peak. Figures 1, 2, and 3 show

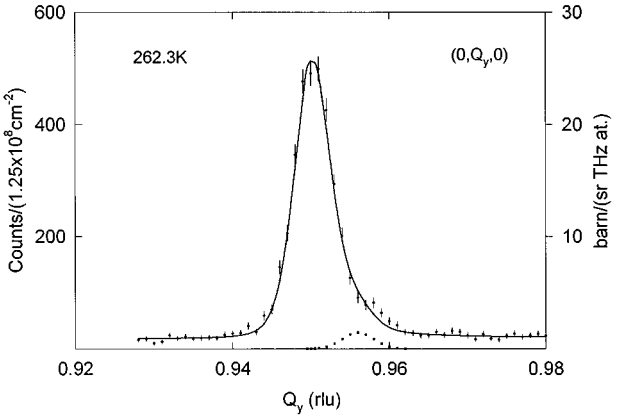

FIG. 1. Part of a radial elastic scan across $(0,1-\delta,0)$ at 262.3 ± 0.1 K. The solid line is the result of the least-squares fit of the resolution-folded Sato-Maki critical scattering model plus weak impurity-phase Bragg scattering to all of the data at this temperature, as described in the text. The dotted line shows the contribution of the impurity-phase Bragg peak.

elastic, constant-E, and constant-**Q** data at 262.3 K (1.2 K above the transition). In those figures, the left-hand scale is the observed counts at the indicated neutron exposures (per unit area), while the right-hand scale is intensity normalized to phonons in the sample and vanadium incoherent scattering. The elastic scan peaks (e.g., Fig. 1) are broader than

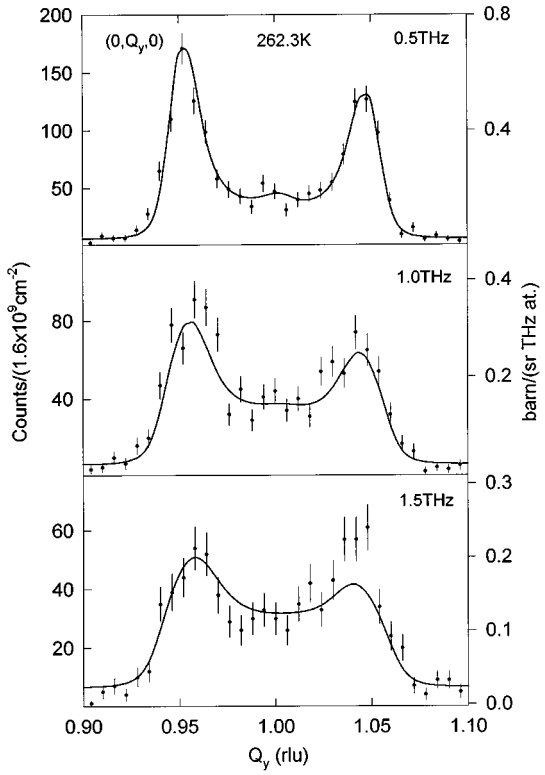

FIG. 2. Radial constant-E scans, at the energy transfers indicated, across $(0,1\pm\delta,0)$ and (010) at 262.3 ± 0.1 K. The solid lines are the result of the least-squares fit of the resolution-folded Sato-Maki critical scattering model (plus weak impurity-phase Bragg scattering) to all of the data at this temperature, as described in the text.

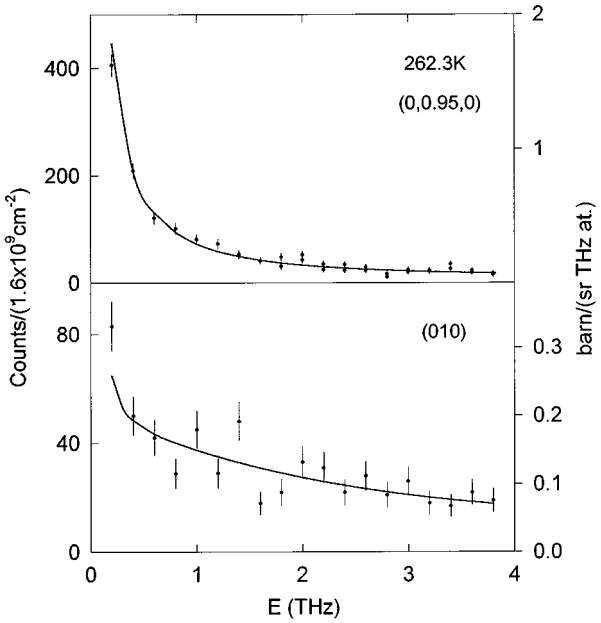

FIG. 3. Constant-**Q** scans, at the positions indicated, at 262.3 ± 0.1 K. The solid lines are the result of the least-squares fit of the resolution-folded Sato-Maki critical scattering model (plus weak impurity-phase Bragg scattering) to all of the data at this temperature, as described in the text.

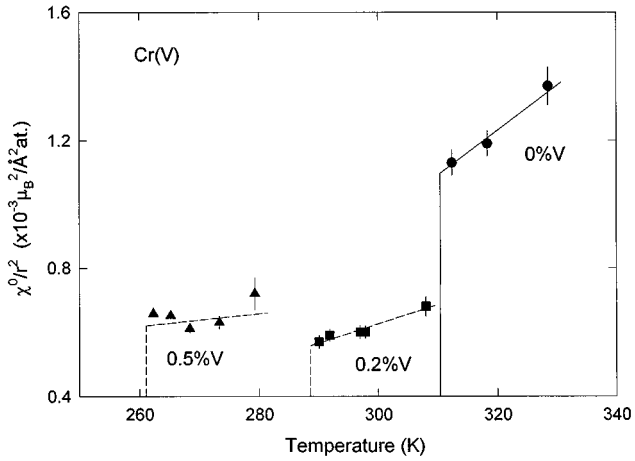

FIG. 4. Amplitude scale χ^0/r^2 deduced from least-squares fits of the Sato-Maki critical scattering model to triple-axis neutron scattering data at the temperatures shown in the samples indicated. The lines are guides for the eye (the vertical lines show the samples' respective Néel temperatures).

Bragg peaks, and have weak shoulders on their more-commensurate sides due to the impurity-phase Bragg scattering. Similar scans at nonzero energy transfer (Fig. 2) show much broader peaks, with considerable additional observed intensity between the peaks (that is, around the commensurate position). Much of this intensity is contributed by the corresponding broad peaks above and below the spectrometer plane $(0,1,\pm\delta)$, critical scattering from which is collected between the in-plane incommensurate peaks by the relatively poor vertical resolution which is a normal design feature of triple-axis spectrometers.

IV. ANALYSIS: RESOLUTION-FOLDED FITTING

The theoretical cross section must be convoluted (''folded'') with the spectrometer resolution function to produce the ''predicted spectrometer response'' that can be directly compared to the data. The resolution function was calculated by the method of Cooper and Nathans,[16] as described in Ref. 14. The elements of the resolution function were determined from the mosaic spreads of the monochromator (0.20°) and analyzer (0.15°), and collimator divergence angles in the horizontal spectrometer plane (0.73°-0.53°-0.56°-2.5°) and in the vertical direction (0.93°-1.2°-2.1°-7.1°). A sample mosaic spread of 0.20° provided the best match between the calculated and observed half-height contour of the $(0,1-\delta,0)$ magnetic Bragg peak at 254 K (7 K below the transition). With this parametrization of the Cr +0.5 at. % V experiment, simulations folding the resolution function with the known dispersion curves of phonons in chromium produced good agreement with the observed constant-**Q** scans over phonons around (020) used for intensity calibration.

To fit theory to the data, the theoretical Sato-Maki cross section was folded numerically with the spectrometer resolution in a least-squares fitting, in the manner of Ref. 14. For each temperature set, all data taken (elastic and inelastic) were fit simultaneously. A separate Bragg scattering signal, representing the impurity phase, was added to the critical scattering model of the majority phase. The complete fit function also included independent terms for incoherent elastic scattering from the sample and energy-independent stray random background. The results of the fit to the 262.3 K data are shown as the solid lines on Figs. 1–3. The impurity-phase Bragg scattering makes a noticeable contribution only to the elastic scan (Fig. 1, where the dotted line explicitly shows it), and even there it is small for temperatures near the majority-phase transition. Sets of data at temperatures up to 279.3(2) K were analyzed using this model, with consistent, reasonable results. Data were also taken at 291 K, but fits of the Sato-Maki model to those data produced parameter values inconsistent with the values from lower temperatures. Since this was only a few degrees below the Néel temperature of the impurity phase, we concluded that critical scattering from the impurity phase had become strong enough to compete with critical scattering from the majority phase at this temperature, making detailed analysis impossible.

The Sato-Maki parameters deduced from the fits are (χ^0/r^2), the amplitude scale; κ^2, the inverse correlation length squared; A^2, the magnetic stiffness; and δ, the paramagnetic incommensurability. The results for the first three are summarized in plots versus measurement temperature in Figs. 4, 5, and 6, respectively, along with the results of fitting the Sato-Maki model to similar data on chromium and Cr +0.2 at. % V reported previously.[13] Note that Fig. 5 is a log-log plot with respect to reduced temperature $\tau \equiv (T-T_N)/T_N$, while the other three figures are linear-scale plots versus absolute temperature. δ values were consistent with the well-known trends of that parameter as temperature and vanadium concentration are varied.[1]

V. DISCUSSION

If the Sato-Maki critical scattering model is to be fully consistent with the data, then the temperature dependence of

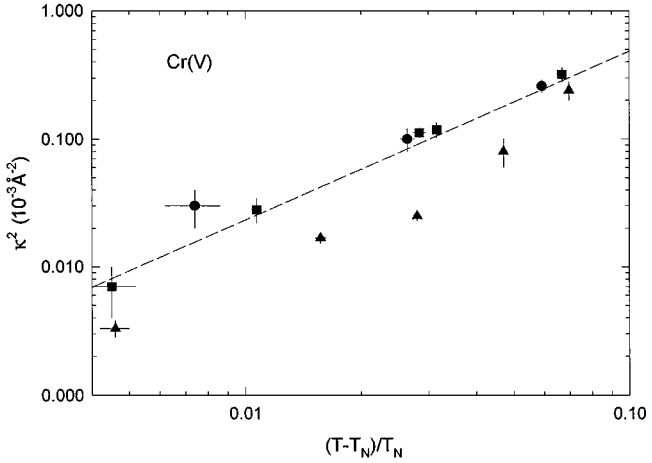

FIG. 5. κ^2, the square of the inverse correlation length, deduced from least-squares fits of the Sato-Maki critical scattering model to triple-axis neutron scattering data as a function of reduced temperature for pure chromium (circles), Cr+0.2 at. % V (squares), and Cr+0.5 at. % V (triangles). The line is a guide for the eye (it has slope 1.36).

the scattering should be almost entirely in temperature dependence of κ, the reciprocal of the correlation length. In a commensurate ordering, the ordering wave vector, and hence the peak of critical scattering intensity, is perforce locked to the crystalline lattice, but in this incommensurate case there is no strong argument for fixing it in place. The critical analysis would be simpler if the paramagnetic incommensurability δ was fixed, but it is well known that the magnetic Bragg incommensurability is temperature dependent right up to T_N, and that is generally interpreted to mean that the Fermi surface nesting responsible for the ordering is changing slightly with temperature. If the temperature dependence of the nesting continues in the paramagnetic state, then δ should be temperature dependent. Then χ^0/r^2 and A^2, which may also depend on nesting, may also vary with temperature. These ''nesting temperature dependences'' are fairly gentle

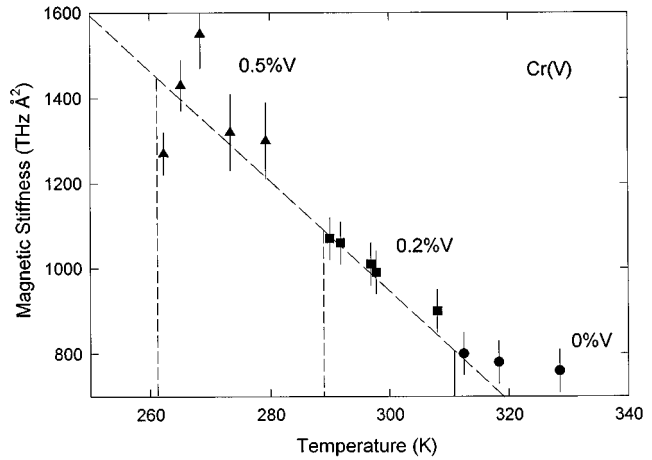

FIG. 6. The magnetic stiffness A^2 deduced from least-squares fits of the Sato-Maki critical scattering model to triple-axis neutron scattering data at the temperatures shown in the samples indicated. The lines are guides for the eye (the vertical lines show the samples' respective Néel temperatures).

by comparison with the critical variation of κ^2. As can be seen in Fig. 5, then, for each sample, κ^2 goes through orders of magnitude change over the temperature ranges studied, while δ is known to decrease only slightly as temperature is raised (as does the Bragg incommensurability below T_N).[1,3] We now see that there is also some temperature variation in the susceptibility amplitude scale (χ^0/r^2, Fig. 4) and stiffness (A^2, Fig. 6).

Changing vanadium concentration shifts the Fermi energy, and thus the nesting, resulting in the well-known concentration dependence of the ordering wave vector and Néel temperature.[3] Figures 4–6 indicate the effect of vanadium concentration on the Sato-Maki parameters of the paramagnetic critical scattering. Figure 5 actually shows that triple-axis scattering is too slow in acquiring data (with today's technology) to be good for determination of the critical exponent for ν. The line drawn in the figure indicates a general trend with slope (2ν) near 1.4, but we consider this only a crude indication of the critical exponent. There seems to be no distinction between pure chromium and Cr+0.2 at. % V, and the Cr+0.5 at. % V data, while displaced downward, are consistent with the same slope. A ν value near 0.7 is reasonable for a magnetic system with three-dimensional interactions.[17]

In Fig. 4, the Sato-Maki model amplitude scale χ^0/r^2, after dropping by more than a factor of 2 when 0.2 at. % V was added to chromium,[18] changes little with the further addition of vanadium to 0.5 at. %, perhaps increasing slightly (uncertainty in the relative volume of the impurity phase in this last sample adds systematic uncertainty of about 10% to the statistical uncertainties shown for this sample's amplitude). This amplitude scale represents a combination of the strength (χ^0) of the magnetism upon which the ordering interaction builds and the range (r) of that interaction, and is associated with the particular model of **Q** and E dependence used to analyze the data. It has been suggested that the rapid drop in amplitude scale on the first introduction of vanadium is associated with the decrease in the nuclear spin-lattice relaxation rate and the electrical resistivity, and perhaps also with the recently discovered formation of local moments, in dilute Cr(V) alloys.[19] Remember that the tricritical point also lies between pure chromium and 0.2 at. % V,[12] and so there is scope for subtle effects to occur in this region.

Finally, Fig. 6 displays the magnetic stiffness A^2, which governs how broad in energy the critical scattering is, a property that can only be measured in an energy-resolved experiment. $A^2(T)$ roughly follows a straight line of negative slope: As the sample Néel temperature decreases, the energy range of paramagnetic critical fluctuations becomes wider. We expect this trend to continue to higher vanadium concentration, even past the cutoff concentration (slightly below 4 at. % V) where T_N goes to zero. Beyond that, no long-range magnetic ordering occurs, but incommensurate magnetic correlations (''SDW paramagnons'') have been observed in a single crystal of Cr+5 at. % V, and they extend to much higher energies than the data from the samples reported here.[20,21] While our current analysis cannot be extrapolated past the cutoff concentration (the interaction enhancement goes to zero as the ordering temperature goes to zero), the similarity in the form of the observed neutron scattering

across the cutoff strongly suggests that there should be a common explanation.

VI. CONCLUSION

Critical neutron scattering was observed in a single crystal of Cr+0.5 at. % V, from near 1 K above the Néel transition at $T_N = 261.1 \pm 0.1$ K to near 18 K above it. At each of five observation temperatures, all the data (elastic and inelastic) were fit well by a magnetic critical scattering model by use of a form of susceptibility (originally proposed by Sato and Maki) that explicitly incorporates the symmetry around the (100) position that the nearly commensurate critical correlations and excitations must respect. This model was previously shown to fit similar data from pure chromium and Cr+0.2 at. % V. The results are roughly consistent with a critical exponent ν near 0.7, for the inverse correlation range. The magnetic stiffness appears to evolve smoothly with vanadium concentration over the range studied, but the Sato-Maki amplitude scale, after dropping by more than a factor of 2 across the region of the tricritical point (and the onset of local moments) between pure chromium and 0.2 at. % V, then changes little with the further addition of vanadium to 0.5 at. %. The similarity in the observed scattering in these samples to the ''SDW paramagnons'' observed in strictly paramagnetic Cr+5 at. % V suggests they should have a common explanation, but the current model requires that ordering occur, and so cannot be extended past the cutoff vanadium concentration where the SDW disappears.

ACKNOWLEDGMENTS

This work was supported in part by U.S. DOE Grant No. DE-FG05-88ER45353 and the NSERC of Canada.

[1] For a review of the magnetism of pure chromium, see E. Fawcett, Rev. Mod. Phys. **60**, 209 (1988).

[2] W.M. Lomer, Proc. Phys. Soc. London **80**, 489 (1962).

[3] For a review of the magnetism of chromium-rich alloys, see E. Fawcett, H.L. Alberts, V.Y. Galkin, D.R. Noakes, and J.V. Yakhmi, Rev. Mod. Phys. **66**, 25 (1994).

[4] For example, B.J. Sternlieb, E. Lorenzo, G. Shirane, S.A. Werner, and E. Fawcett, Phys. Rev. B **50**, 16 438 (1994); S.M. Dubiel, J. Magn. Magn. Mater. **124**, 31 (1993), and references cited in Ref. 3.

[5] H. Sato and K. Maki, Int. J. Magn. **6**, 183 (1974).

[6] R.S. Fishman and S.H. Liu, Phys. Rev. B **45**, 12 306 (1992); **47**, 11 870 (1993); **48**, 3820 (1993); J. Phys. Condens. Matter **5**, 3959 (1993); J. Magn. Magn. Mater. **125**, L1 (1993); Int. J. Mod. Phys. B **7**, 620 (1993); J. Appl. Phys. **75**, 6290 (1994).

[7] A.S. Arrott, S.A. Werner, and H. Kendrick, Phys. Rev. Lett. **14**, 1022 (1965); S.A. Werner, A.S. Arrott, and H. Kendrick, Phys. Rev. **155**, 528 (1967).

[8] C.R. Fincher, G. Shirane, and S.A. Werner, Phys. Rev. Lett. **43**, 1441 (1979); S.K. Burke, W.G. Stirling, K.R.A. Ziebeck, and J.G. Booth, *ibid.* **51**, 494 (1983); B.J. Sternlieb, G. Shirane, S.A. Werner, and E. Fawcett, Phys. Rev. B **48**, 10 217 (1993).

[9] C.R. Fincher, G. Shirane, and S.A. Werner, Phys. Rev. B **24**, 1312 (1981); B.H. Grier, G. Shirane, and S.A. Werner, *ibid.* **31**, 2892 (1985).

[10] B.J. Sternlieb, J.P. Hill, T. Inami, G. Shirane, W.T. Lee, S.A. Werner, and E. Fawcett, Phys. Rev. Lett. **75**, 541 (1995).

[11] J. Als-Nielsen, J.D. Axe, and G. Shirane, J. Appl. Phys. **42**, 1666 (1971).

[12] E. Fawcett, R.B. Roberts, R. Day, and G.K. White, Europhys. Lett. **1**, 473 (1986); P.C. de Camargo, E.P. Castro, and E. Fawcett, J. Phys. F **18**, L219 (1988); E. Fawcett and D.R. Noakes, Int. J. Mod. Phys. B **7**, 624 (1993).

[13] D.R. Noakes, T.M. Holden, E. Fawcett, and P.C. de Camargo, Phys. Rev. Lett. **65**, 369 (1990); D.R. Noakes, T.M. Holden, and E. Fawcett, J. Appl. Phys. **67**, 5262 (1990); E. Fawcett, T.M. Holden, and D.R. Noakes, Physica B **174**, 18 (1991).

[14] T.M. Holden, W.J.L. Buyers, E.C. Svensson, and G.H. Lander, Phys. Rev. B **26**, 6227 (1982).

[15] T. Izuyama, D.J. Kim, and R. Kubo, J. Phys. Soc. Jpn. **18**, 1025 (1963).

[16] M.J. Cooper and R. Nathans, Acta Crystallogr. **23**, 357 (1967); S.A. Werner and R. Pynn, J. Appl. Phys. **42**, 4736 (1971).

[17] H.E. Stanley, *Introduction to Phase Transitions and Critical Phenomena* (Oxford University Press, New York, 1971).

[18] E. Fawcett, J. Phys. Condens. Matter **4**, 923 (1992); Physica **180-181**, 179 (1992).

[19] P. Hill, N. Ali, A.J.A. de Oliveira, W.A. Ortiz, P.C. de Camargo, and E. Fawcett, J. Phys. Condens. Matter **6**, 1761 (1994).

[20] E. Fawcett, S.A. Werner, A. Goldman, and G. Shirane, Phys. Rev. Lett. **61**, 558 (1988); Physica B **156**, 715 (1989); S.A. Werner, E. Fawcett, M.W. Elmiger, and G. Shirane, J. Appl. Phys. **73**, 6454 (1993).

[21] S.M. Hayden, R. Doubble, T.G. Perring, G. Aeppli, and E. Fawcett, Physica B (to be published).